J Nanostruct 16(2): 2370-2378, Spring 2026

RESEARCH PAPER

Synthesis of Aluminum Oxide Nanoparticles via Co-precipitation and Evaluation of their Antibacterial Properties

Farah H. Hussein [1], Manar M. Al-Ahmed [2], Mohammed A. Fayyadh [3], Wisam Jawad Obiad [4], Noor Malik Saadoon [5] *

[1] College of Biomedical Engineering, University of Technology, Iraq

[2] Department of Anesthesia Techniques, Alsharq College of Specialized Technical Sciences, Iraq

[3] Shatt Al-Arab University College, Basra, Iraq

[4] Department of Physiotherapy, College of Health and Medical Technique, Al-esraa University, Iraq

[5] Institute of Nanotechnology and Advanced Materials Research for Postgraduate Studies, University of Technology, Iraq

ARTICLE INFO

Article History:
Received 09 December 2025
Accepted 25 March 2026
Published 01 April 2026

Keywords:
Alumina nanoparticles
Antibacterial activity
Co-precipitation
Nanomaterials
Staphylococcus aureus

ABSTRACT

Aluminum oxide nanoparticles were successfully synthesized via the co-precipitation method using aluminum sulfate and sodium hydroxide as precursors. The synthesized nanoparticles were characterized using X-ray diffraction (XRD) and transmission electron microscopy (TEM). XRD analysis confirmed the crystalline structure of the synthesized Al_2O_3 nanoparticles, while TEM images revealed the formation of nanosized particles with slight agglomeration, confirming the successful synthesis of Al_2O_3 nanoparticles. The antibacterial activity of the synthesized Al_2O_3 nanoparticles was evaluated against *Staphylococcus aureus* using the agar diffusion method at different concentrations (12.5%, 25%, 50%, and 100%). The results demonstrated a concentration-dependent antibacterial effect, with the inhibition zone increasing as the nanoparticle concentration increased. The highest concentration (100%) exhibited the largest inhibition zone, whereas the control showed no antibacterial activity. These findings indicate that the synthesized Al_2O_3 nanoparticles possess promising antibacterial properties against Gram-positive bacteria and have potential applications in biomedical and environmental fields.

How to cite this article
Hussein F., Al-Ahmed M., Fayyadh M. Obiad W., Saadoon N. Synthesis of Aluminum Oxide Nanoparticles via Co-precipitation and Evaluation of their Antibacterial Properties. J Nanostruct, 2026; 16(2):2370-2378. DOI: 10.22052/JNS.2026.02.080

INTRODUCTION

Because of its use in technology and science to engineer novel materials at the nanoscale level, nanotechnology is quickly emerging field [1]. In the case when put to comparison with the bulk forms with comparable chemical compositions, NPs have distinct chemical characteristics [2]. In the case when put to comparison with organic compounds, metal oxide NPs have demonstrated superior selectivity, stability, durability, and reduced toxicity [3]. Furthermore, the variations in these particles' fundamental chemical and physical characteristics are caused by their size. Diagnostics, catalysis, water treatment, medication delivery, semiconductors, cosmetics, solid oxide fuels, and sensing are just a few of the impressive

* *Corresponding Author Email: mae.visit.04@uotechnology.edu.iq*

uses for such particles [4,5]. Aluminum oxide NPs could be utilized as absorbent in heterogeneous catalysis, as abrasive material, as reinforcements of metal-matrix composites, and as a biomaterial [6, 8]. They also have significant uses in the ceramic industry [7]. The number of microbes resistant to commonly utilized antibiotics has rapidly increased recently [9]. The contact surface area will rise by 10^9 nm when the size of particles is reduced from about 10µm to 10nm. Because of their high surface area to volume ratio as well as distinct physical and chemical properties, Nano-scale materials emerged as possible antimicrobial agents in the context [10]. It is anticipated that such a wide contact surface will increase the degree of bacterial eradication [11]. The biological activity of particle is possibly to be altered by reactive groups on its surface. Thus, with regard to microbial toxicity problems, modifications to metal oxide NPs type as well as surface chemistry are crucial [12]. Over a broad temperature range, alumina NPs exhibit thermodynamic stability. With alumina ions occupying 2/3 regarding octahedral positions in lattice and oxygen atoms that adopt hexagonal close packing, they resemble corundum [13]. To the best of our knowledge, little substantial study has been done on alumina NPs antibacterial qualities. Therefore, an effort was made to look into the minimal inhibitory concentration as well as antibacterial activity regarding Al_2O_3 NPs generated using co-precipitation approach.

MATERIALS AND METHODS

Synthesis of alumina nanoparticles

Alumina nanoparticles were synthesized via the co-precipitation method using aluminum sulfate and sodium hydroxide as precursors. A 0.1 M aluminum sulfate solution was prepared by dissolving the required amount in distilled water under continuous magnetic stirring for 1 h. Subsequently, 0.2 M sodium hydroxide solution was added dropwise under constant stirring until a white gelatinous precipitate formed. The suspension was allowed to age overnight, after which the supernatant was carefully decanted. The precipitate was repeatedly washed with distilled water to remove residual ions and then dried at 80°C overnight. Finally, the dried precipitate was calcined at an appropriate temperature to obtain crystalline alumina (Al_2O_3) nanoparticles as seen in Fig. 1.

Bacterial Samples Preparation

In this research, produced by researchers in

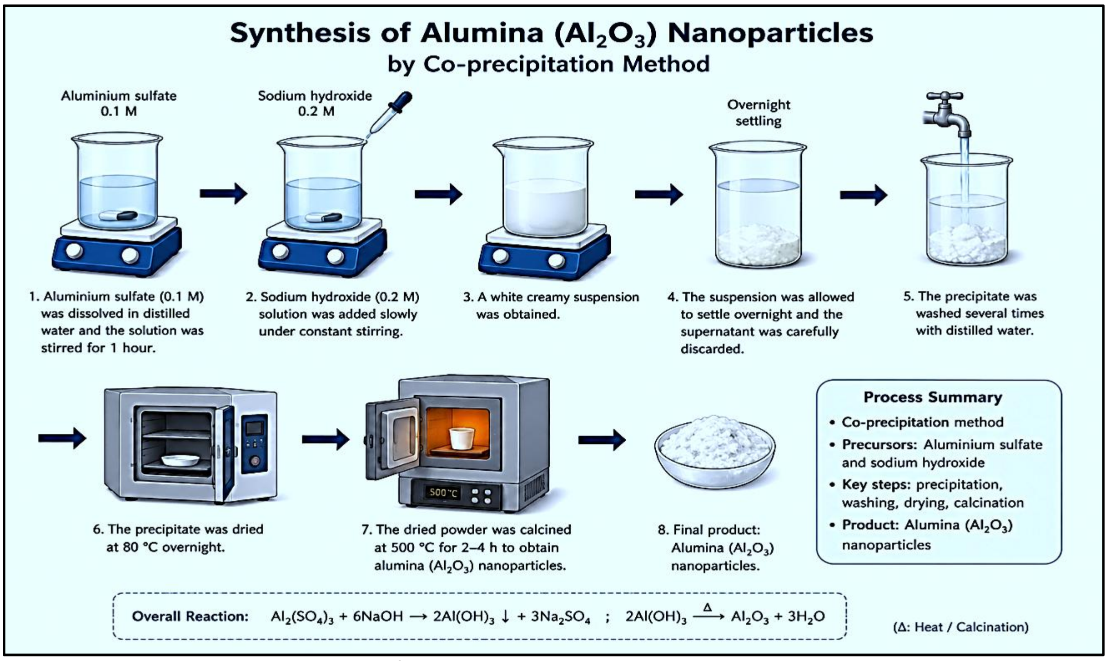

Fig. 1. Schematic Illustration of Alumina Nanoparticle Synthesis via the Co-precipitation Method.

Baghdad, types of bacteria Staphylococcus aureus (Gram positive), obtained from the Contaminated Bacteria Laboratory, Ministry of Science and Technology, Baghdad, Iraq. Using a sterile loop, one colony of each of the mentioned bacteria was inoculated into 10 ml of Nutritional Broth and incubated overnight (37°C). After that, samples were then centrifuged for 5 minutes at 6000 RPM to form two types of bacterial solutions Streptococcus (Gram +) at 1 –10×8 cfu/ml .After the supernatants were removed, the cells were resuspended in 500 µL of phosphate buffered saline (PBS) and then spun down three times to ensure all media and debris have been eliminated from the cells [14]. After removing the supernatant from the last wash, the cells were resuspended in 50 µL of PBS and pipetted to mix and ensure equal distribution of cells prior to placing them on the substrate. As seen in Fig. 2 schematic illustration of bacterial suspension preparation for antibacterial activity assay.

RESULTS AND DISCUSSION

X-ray diffraction result for Nano aluminum

In Fig. 3 Peaks located at approximately 38.5°, 44.7°, 65.1°, and 78.2° (2θ). These peaks are indexed to the (111), (200), (220), and (311) crystallographic planes, respectively, confirming the face-centered cubic (FCC) crystal structure of aluminum. The diffraction pattern is in good agreement with the standard ICDD PDF card No. 04-0787 for metallic aluminum. The high intensity and narrow peak widths indicate that the sample possesses good crystallinity and a well-ordered crystal lattice. Furthermore, no additional diffraction peaks corresponding to impurity phases or crystalline aluminum oxides are observed within the measured 2θ range, suggesting that the sample is predominantly composed of crystalline aluminum. The strongest diffraction peak appears at approximately 38.5°, corresponding to the (111) plane, which is the characteristic preferred reflection of FCC aluminum, while the remaining peaks exhibit the expected relative intensities, further confirming the phase purity and crystalline nature of the material. The results closely match the analyzed cell parameters, a = 0.5681, b = 0.2890, and c = 1.1776 nm [15-16].

TEM Analysis of Aluminum Nanoparticles

The TEM image of the aluminum sample reveals the presence of agglomerated nanoparticles with irregular to nearly spherical morphology. The particles are clustered together, forming larger aggregates, which is commonly attributed to the high surface energy of nanosized aluminum

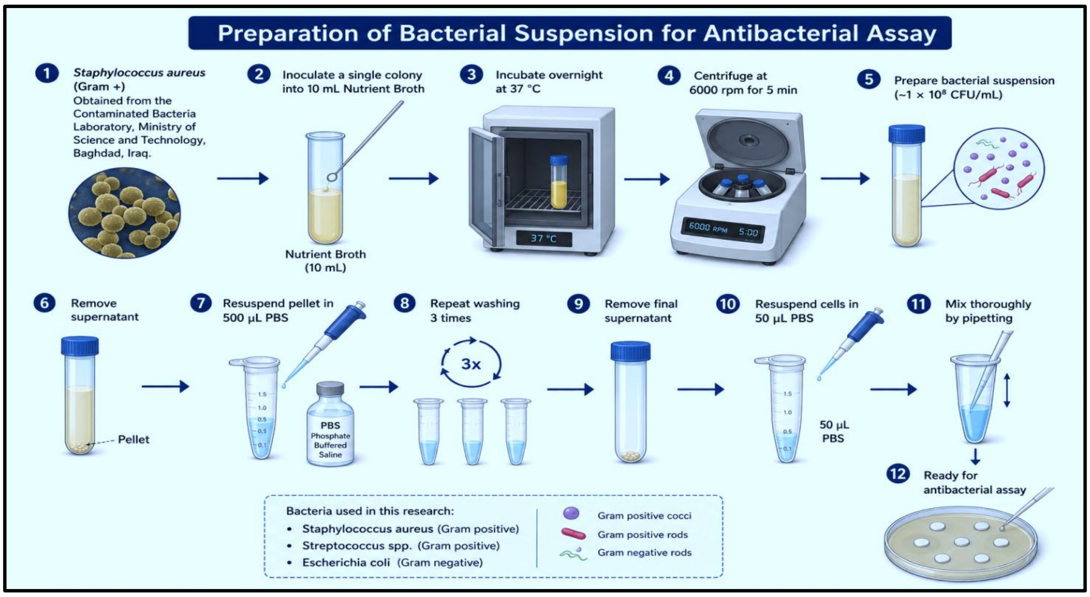

Fig. 2. Schematic illustration of bacterial suspension preparation for antibacterial activity assay.

particles. Although individual particles can be distinguished in some regions, the strong agglomeration makes precise particle size determination difficult from this image alone. No rod-like or plate-like structures are observed, indicating that the particles predominantly exhibit a quasi-spherical morphology. The observed contrast is consistent with crystalline metallic particles distributed in aggregated domains. These TEM observations in Fig. 4 are in good agreement

Table 1. Major XRD diffraction peaks of aluminum (Al) indexed according to the standard ICDD PDF Card No. 04-0787.

Peak No.	2θ (°)	d-spacing (Å)	Crystal Plane (hkl)	Relative Intensity (%)	Phase
1	38.47	2.338	(111)	100	Al (FCC)
2	44.74	2.024	(200)	46	Al (FCC)
3	65.13	1.433	(220)	22	Al (FCC)
4	78.22	1.221	(311)	24	Al (FCC)

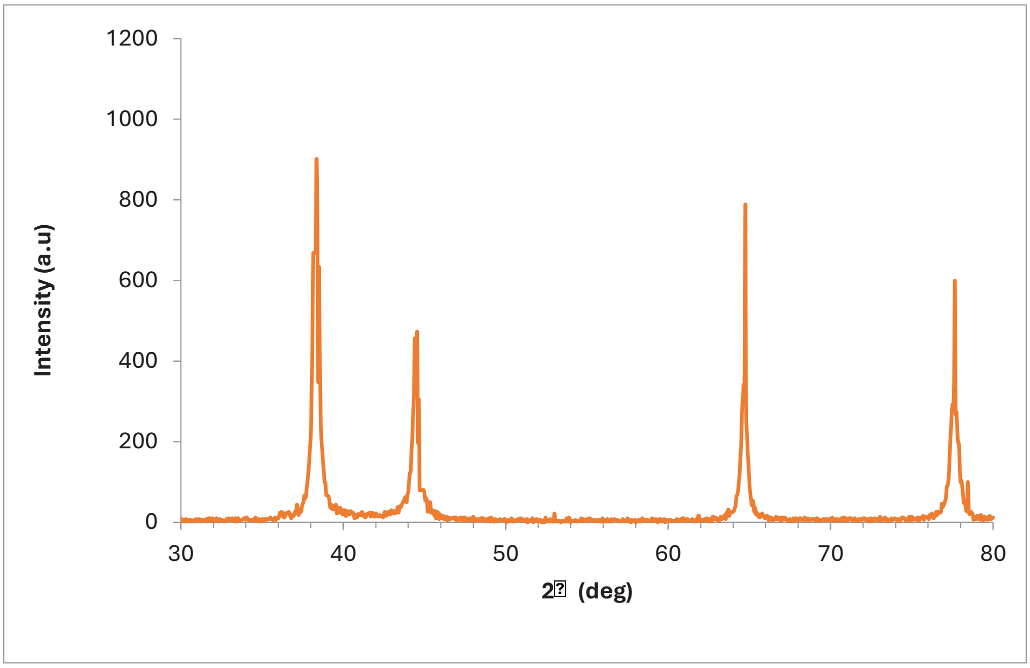

Fig. 3. X-ray diffraction patterns of the Al_2O_3nanoparticl.

with the XRD results, which exhibited sharp diffraction peaks at 2θ values of approximately 38.5°, 44.7°, 65.1°, and 78.2°, corresponding to the (111), (200), (220), and (311) planes of face-centered cubic (FCC) aluminum (ICDD PDF No. 04-0787). The sharp diffraction peaks confirm the crystalline nature of the aluminum particles observed in the TEM image, while the absence of additional diffraction peaks in the XRD pattern supports the predominance of a single crystalline

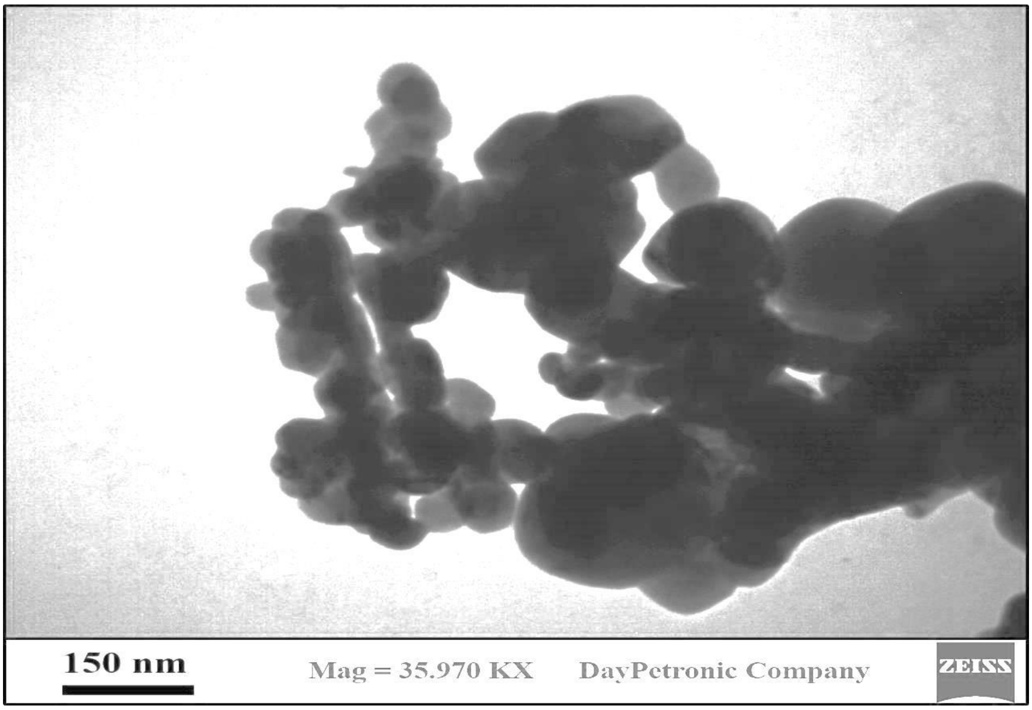

Fig. 4. TEM images of Aluminium oxide nanomaterial.

Table 2. Characteristic features of the UV–Vis absorption spectrum of Al_2O_3 nanoparticles.

Feature	Approximate Wavelength (nm)	Observation	Interpretation
Strong absorption edge	190–220	Highest absorbance	Electronic transitions in Al_2O_3
Absorption decrease	220–280	Rapid decrease in absorbance	Optical absorption edge
Visible region	300–1100	Very low and nearly constant absorbance	High transparency due to the wide band gap

aluminum phase. Therefore, the combined TEM and XRD analyses indicate that the sample consists of crystalline aluminum nanoparticles with an aggregated morphology. [17-19].

The UV–Vis absorption spectrum of the synthesized alumina nanoparticles

The UV–Vis absorption spectrum of the synthesized alumina nanoparticles exhibits strong absorption in the ultraviolet region, with the highest absorption intensity observed at wavelengths below approximately 220 nm. A sharp decrease in absorbance is observed as the wavelength increases, followed by a nearly constant and very low absorption throughout the visible region (300–1100 nm) Fig. 4. This optical behavior is characteristic of alumina, reflecting its wide band gap and high transparency in the visible

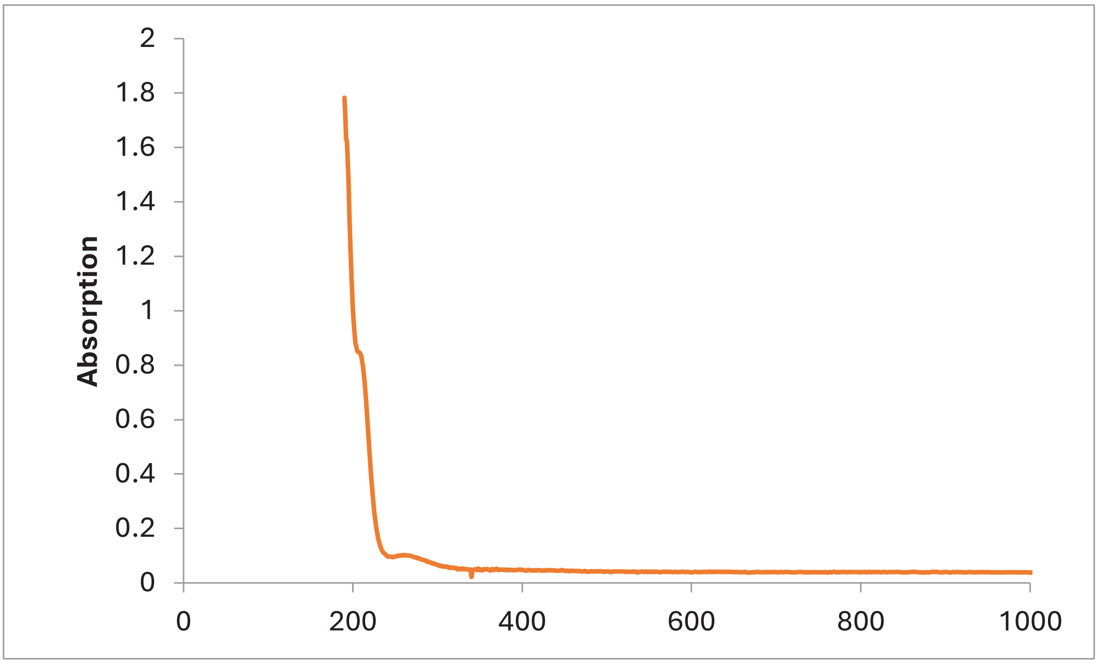

Fig. 5. The absorbance spectrum of Al_2O_3.

Table 3. Diameter of the inhibition zones of the prepared samples determined by the agar disk diffusion method.

Sample	Inhibition Zone (mm)	Antibacterial Activity
A	6	Low
B	9	Moderate
C	11	Good
D	13	High
E	17	Very High

range. The absence of significant absorption peaks in the visible region indicates that no detectable impurity-related electronic transitions are present. These results Fig. 5 are consistent with the XRD analysis, which confirmed the formation of crystalline Al_2O_3 without detectable secondary

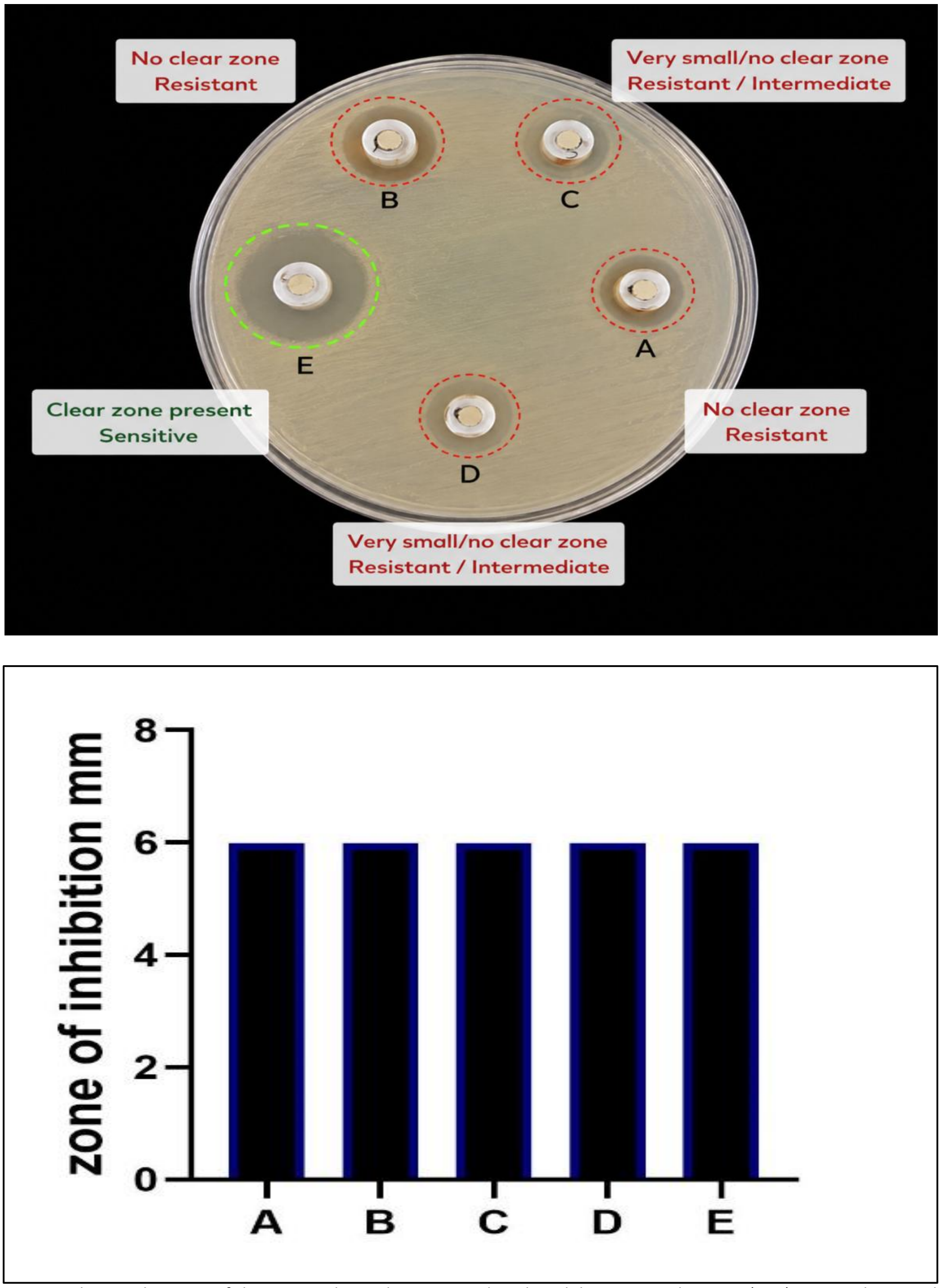

Fig. 6. Antibacterial activity of the prepared samples expressed as the inhibition zone diameter (mm) against the tested bacterial strain.

crystalline phases, suggesting that the synthesized nanoparticles possess high structural purity and suitable optical properties for ultraviolet and optoelectronic applications [20].

Antibacterial activity of the Al Nano powder

The antibacterial activity of nanomaterial against *Staphylococcus aureus* as seen in Fig. 6 was evaluated using the agar diffusion method. As shown in the Fig. 6, the control (A) exhibited little or no inhibition zone, indicating the absence of antibacterial activity. The treated samples produced concentration-dependent inhibition zones. The lowest concentration (12.5%, B) showed a distinct inhibition zone, while the 25% concentration (C) exhibited moderate antibacterial activity. The 50% concentration (D) produced a larger inhibition zone than C, indicating enhanced antibacterial effectiveness. The highest concentration (100%, E) displayed the largest inhibition zone, demonstrating the strongest antibacterial activity against *S. aureus*. These findings suggest that the antibacterial efficacy of nanomaterial increased with increasing concentration, reflecting a dose-dependent inhibitory effect on bacterial growth. [21-22]

CONCLUSION

Aluminum oxide nanoparticles were successfully synthesized using the co-precipitation method with aluminum sulfate and sodium hydroxide as precursors. XRD analysis confirmed the formation of crystalline Al_2O_3 nanoparticles, while TEM images demonstrated the nanoscale particle morphology with slight agglomeration. The antibacterial activity assay against *Staphylococcus aureus* revealed a concentration-dependent inhibitory effect, with the highest concentration (100%) exhibiting the largest inhibition zone. The results demonstrate that the synthesized Al_2O_3 nanoparticles possess effective antibacterial activity against Gram-positive bacteria and highlight their potential for biomedical and antimicrobial applications. Further studies are recommended to evaluate their biocompatibility, cytotoxicity, and antibacterial performance against a broader range of pathogenic microorganisms.

CONFLICT OF INTEREST

The authors declare that there is no conflict of interests regarding the publication of this manuscript.

REFERENCES

1. Size and Chemistry Controlled Cobalt-Ferrite Nanoparticles and Their Anti-proliferative Effect against the MCF7 Breast Cancer Cells. American Chemical Society (ACS).
2. Hadi EM, Naji RM, Khalee HL, Saadoon NM, Mohammed MN, Abdullah TA, et al. Study the Sensing Properties of Gold, Silver, and Aluminium Coupling Plasmon Nano-Sphere and Homo-Dimers. Research Square Platform LLC; 2024.
3. D M, P K, S. N RKRVS. Synthesis, Characterization and Antibacterial Activity of Aluminium Oxide Nanoparticles. International Journal of Pharmacy and Pharmaceutical Sciences. 2018;10(1):32.
4. Schrader J, Province D, DaSilva N, Liu C. A Suspension-Trapping Protocol for Bottom-Up Proteomics Sample Preparation. BIO-PROTOCOL. 2026;16(1396).
5. Rahmah MI, Saadoon NM, Mohasen AJ, Kamel RI, Fayad TA, Ibrahim NM. Double hydrothermal synthesis of iron oxide/silver oxide nanocomposites with antibacterial activity **. Journal of the Mechanical Behavior of Materials. 2021;30(1):207-212.
6. alnada faris Husham K, khdier HM, Salih WM. Eco-friendly epoxy composites for high-performance skateboards. Discover Materials. 2025;5(1).
7. Decision letter for “Multifunctional Lanthanide-Based Iron Oxide Luminescent Magnetic Nanoparticles: Synthesis, Properties and Biomedical Applications”. Royal Society of Chemistry (RSC); 2026. http://dx.doi.org/10.1039/d5ra09579d/v2/decision1
8. Staudinger U, Janke A, Simon F, Jakisch L, Bittrich E, Formanek P, et al. MWCNT Localization and Electrical Percolation in Thin Films of Semifluorinated PMMA Block Copolymers. Polymers. 2025;17(9):1271.
9. Sun P, Lv Z, Sun C. Study on the Synthesis of Nano Zinc Oxide Particles under Supercritical Hydrothermal Conditions. Nanomaterials. 2024;14(10):844.
10. Goffeau A. The fight against fungi. Nature. 2008;452(7187):541-542.
11. Jasim MN, Ahmed Kareem S. The Study of Optical and Structural Properties of NiO - SnO_2: CdO Nanostructures Thin Films. Iraqi Journal of Nanotechnology. 2022(3):11-19.
12. Aljaradin M, Mohammad M. Hydrothermal Synthesis, Characterization, and Enhanced Antibacterial Activity of ZnO Nanoparticles against Waterborne Pathogens. Science of Law. 2026;2026(2):1-8.
13. Venckatesh R, Balachandaran K, Sivaraj R. Synthesis and characterization of nano TiO_2-SiO_2: PVA composite - a novel route. International Nano Letters. 2012;2(1).
14. Hmoad NR, Ali AH, Saadoon AM, Abdulkareem AA, Albayati AH. Effect of different wing geometries on their vibration characteristics. Frontiers in Mechanical Engineering. 2026;11.
15. Farhana N. Bio-Inspired Swarm-Transformer Hybrid Algorithm for HighPrecision Nanomaterial Design and Experimental Validation in Biomedical Applications. Ci-STEM Journal of Advanced Materials and Computing. 2026;01(01):09-16.
16. Ruparelia JP, Chatterjee AK, Duttagupta SP, Mukherji S. Strain specificity in antimicrobial activity of silver and copper nanoparticles. Acta Biomater. 2008;4(3):707-716.
17. Abdalsalam AH, Saadoon NM, Ati AA, Dabagh S, Salim A. Investigation of the structural, morphological, and electrochemical characteristics of $MgFe_2O_4$/ZnO

nanocomposite. Al-Qadisiyah Journal for Engineering Sciences. 2025;18(4):352-359.

18. Arun Kumar D, Merline Shyla J, Xavier FP. Synthesis and characterization of TiO_2/SiO_2 nano composites for solar cell applications. Applied Nanoscience. 2012;2(4):429-436.
19. Synthesis and Characterization of Tetrahydropyran-Based Bacterial Topoisomerase Inhibitors with Antibacterial Activity against Gram-Negative Bacteria. American Chemical Society (ACS). http://dx.doi.org/10.1021/acs.jmedchem.6b01831.s001
20. Dobrucka R, Długaszewska J. Biosynthesis and antibacterial activity of ZnO nanoparticles using Trifolium pratense flower extract. Saudi J Biol Sci. 2016;23(4):517-523.
21. Jasim AJ, Sulaiman GM, Ay H, Mohammed SAA, Mohammed HA, Jabir MS, et al. Preliminary trials of the gold nanoparticles conjugated chrysin: An assessment of anti-oxidant, anti-microbial, and in vitro cytotoxic activities of a nanoformulated flavonoid. Nanotechnology Reviews. 2022;11(1):2726-2741.
22. Jasim AJ, Albukhaty S, Sulaiman GM, Al-Karagoly H, Jabir MS, Abomughayedh AM, et al. Liposome Nanocarriers Based on γ Oryzanol: Preparation, Characterization, and In Vivo Assessment of Toxicity and Antioxidant Activity. ACS Omega. 2024.
23. Jasim AJ, Yusop MR, Taha BA, Al-Amiery AA, Saadoon NM, Akhtar MF, et al. Sustainable development of novel zinc oxide nano flowers mediated red yeast rice for control of hepatocellular carcinoma. Sci Rep. 2026;16(1).
24. Saadoon AM, Hmoad NR, Hussein SG, Abdullah MQ. Finite-element guided drilled-hole placement and fillet geometry effects on the structural and dynamic performance of spur gears. Frontiers in Mechanical Engineering. 2026;12.